

# A Novel Enzyme-Free Hydrogen Peroxide Sensor Based on Electrode Modified with Gold Nanoparticles-Overoxidized Polydopamine Composites

Su-Juan Li<sup>\*</sup>, Lin-Lin Hou, Meng-Zhu Chang, Juan-Juan Yan, Lin Liu

Key Laboratory for Clearer Energy and Functional Materials of Henan Province, College of Chemistry and Chemical Engineering, Anyang Normal University, Anyang, 455000, Henan, China.

\*E-mail: [lemontree88@163.com](mailto:lemontree88@163.com)

Received: 12 January 2016 / Accepted: 1 February 2016 / Published: 1 March 2016

---

A new electrode was fabricated by electrodeposition of gold nanoparticles (Au NPs) on overoxidized polydopamine (OPDA) modified gold electrode. The integration of Au NPs and the OPDA film endowed the Au NPs/OPDA modified electrode with high sensitivity and selectivity and good electrocatalytic activities to reduction of hydrogen peroxide ( $\text{H}_2\text{O}_2$ ). Compared to electrodes modified with individual Au NPs or OPDA films, the Au NPs/OPDA modified electrode presents the largest current response to reduction of  $\text{H}_2\text{O}_2$ , due to a possible synergism between the OPDA film and the Au NPs. The proposed  $\text{H}_2\text{O}_2$  sensor has a response sensitivity of  $52.94 \mu\text{A mM}^{-1} \text{cm}^{-2}$  and a wide linear range from  $10 \mu\text{M}$  to  $8 \text{mM}$ . The detection limit is estimated to be  $0.5 \mu\text{M}$ .

---

**Keywords:** Gold nanoparticles; Polydopamine; Electrodeposition; Hydrogen peroxide

## 1. INTRODUCTION

The fast and precise determination of  $\text{H}_2\text{O}_2$  is of importance due to the fact that  $\text{H}_2\text{O}_2$  generates the diagnostic response for blood glucose monitoring devices [1]. Meanwhile,  $\text{H}_2\text{O}_2$  plays a crucial role in many fields including food control, the textile industry, fuel cell devices and environmental protection. To date, various effective strategies have been proposed for detection of  $\text{H}_2\text{O}_2$  [2-9]. Among these strategies, electrochemical technique is one of the most commonly used methods due to its comparatively high sensitivity, low cost, good selectivity and simple manipulation. The enzymatic and enzyme-free based electrochemical methods were often used as  $\text{H}_2\text{O}_2$  sensors. Strict experimental conditions are always needed for enzymatic based sensors due to the vulnerable activities of enzymes [10,11]. Moreover, this type of sensors cannot function with good reproducibility and long-term

stability. Therefore, it needs urgently to develop enzyme-free  $\text{H}_2\text{O}_2$  sensors with low detection limit and high detection sensitivity. Among the enzyme-free  $\text{H}_2\text{O}_2$  sensors, Prussian blue (PB), characterized with enhanced enzyme-mimetic properties, is commonly used to detect  $\text{H}_2\text{O}_2$  based on its excellent electrocatalytic activity toward reduction of  $\text{H}_2\text{O}_2$  [12]. Unfortunately, the decomposition of PB film in neutral and alkaline solutions limits its catalytic efficiency and widespread application. The use of nanostructured materials is another promising strategy to construct nonenzymatic  $\text{H}_2\text{O}_2$  sensor. Various nanostructured metals and their oxides, such as Pt [13], Au [14,15], Ag [16,17],  $\text{CoO}_x$  [18,19],  $\text{MnO}_2$  [20,21] and  $\text{Cu}_2\text{O}$  [22], have been utilized as electrode modifications for sensing of  $\text{H}_2\text{O}_2$ .

Recently, Gold nanoparticles (Au NPs) have aroused intensive research interest in the fields of chemically modified electrodes. It has been proved that Au NPs have the capability to enhance the electrical conductivity, promote the electron transfer and increase the detection sensitivity of electrode [23]. Therefore, Au NPs have been widely used as electrocatalysts for biosensing applications. Importantly, the properties of substrate electrode for immobilization of Au NPs is vital because it influence the electrocatalytic performance of Au NPs [24,25]. Very recently, polymers especially polydopamine (PDA) provide an avenue for loading and stabilizing metal nanoparticles as the supporting materials. PDA has many attractive features, for example PDA films can be formed on various substrates including organic and inorganic materials that allow for the subsequent modification. So far, PDA has been successfully used as a catalyst support in many catalytic systems [13,17,25,26]. Furthermore, the PDA film is capable of undergoing further over-oxidization at positive potentials to form the over-oxidized polydopamine (OPDA) [27,28], resulting in a rough and loose structure to facilitate immobilization of metal nanoparticles and thus generates additional electrocatalytic sites.

In this work, dopamine was electropolymerized on a gold substrate electrode in 60 mM phosphate buffer solutions (pH 7.0). For overoxidizing the electropolymerized dopamine film, the modified electrode was electrocycled in 0.5 M NaOH solution. The synthesized OPDA films exhibited high electrochemical activity and stability on gold electrode. The obtained OPDA modified gold electrode was used as substrate for Au NPs electrochemical deposition, on which the  $\text{H}_2\text{O}_2$  electroreduction was investigated at the resultant Au NPs/OPDA modified gold electrode (Au NPs/OPDA/Au). Here, the detection of  $\text{H}_2\text{O}_2$  by cathodic reduction was performed to avoid the interferences of coexisting substance in physical samples. The as-fabricated Au NPs/OPDA based non-enzymatic  $\text{H}_2\text{O}_2$  sensor exhibited excellent electrocatalytic activities towards the rapid sensing of  $\text{H}_2\text{O}_2$  over a wide linear range from 10  $\mu\text{M}$  to 8 mM.

## 2. EXPERIMENTAL SECTION

### 2.1. Reagents and apparatus

Dopamine was obtained from Sigma-Aldrich.  $\text{HAuCl}_4 \cdot 4\text{H}_2\text{O}$ ,  $\text{H}_2\text{O}_2$  and all other chemicals were purchased obtained from Beijing Chemical Factory. The supporting electrolyte was prepared

from the salts  $\text{Na}_2\text{HPO}_4$  and  $\text{KH}_2\text{PO}_4$  to a 60 mM phosphate buffer solution (PBS, pH 7.0). Unless otherwise stated.

Scanning electron microscopy (SEM) was conducted by Hitachi SU8010 (Hitachi, Japan) for observations of surface morphology of electrode. Electrochemical measurements were carried out on a CHI 660D electrochemical station (Shanghai Chenhua, China). The electrochemical impedance spectroscopy (EIS) was also conducted using a CHI 660 electrochemical station in 5 mM  $\text{Fe}(\text{CN})_6^{3-/4-}$  with 0.1 M KCl involved as supporting electrolyte in the frequency range of  $10^5$ -0.1 Hz. The conventional three-electrode system included the Au NPs/OPDA modified gold working electrode, a Pt wire counter electrode and a saturated calomel reference electrode (SCE).

## 2.2. Preparation of Au NPs/OPDA modified electrode

Before usage, a bare gold electrode (2 mm diameter) was polished on a polishing cloth with 1.0, 0.3 and 0.05  $\mu\text{m}$  alumina powder respectively and rinsed with deionized water between each polishing step and sequentially sonicated in acetone, ethanol, and deionized water, and then dried at room temperature. Afterwards, the cleaned gold electrode was immersed into electrolytic cell with the deaerated a 5 mM dopamine solution in 60 mM pH 7.0 PBS and cycled under the potential window from -0.6 V to 0.5 V for 25 cycles at a potential scan rate of 0.1 V/s. Then, the modified electrode was taken out from the cell, rinsed with copious water, immersed again into the PBS electrolyte, and cycled under the potential window from -0.6 V to 0.5 V for 20 cycles. For overoxidizing the electropolymerized PDA film, the modified electrode was transferred to the cell with deaerated 0.5 M NaOH solution and cycled 6 times in the potential range from -1.25 V to 0.8 V at a potential scan rate of 0.05 V/s. Here, the OPDA/Au modified electrode was obtained. The subsequent modification of Au NPs was achieved by applying a constant potential of -0.2 V in a deaerated precursor solutions of 0.1 M KCl containing 2.5 mM  $\text{HAuCl}_4$  for a deposition time of 100 s. The OPDA modified gold electrode (OPDA/Au) and Au NPs modified gold electrode (Au NPs/Au) were prepared for comparison experiment, according to their corresponding deposition conditions.

## 3. RESULTS AND DISCUSSION

### 3.1. Formation of the Au NPs/OPDA on gold electrode surface and its morphology characterization

A dopamine polymer was first modified on gold surface by cyclic voltammetry deposition in a 5 mM dopamine solution (pH 7.0). The cyclic voltammograms (CVs) for its deposition are shown in Fig. 1. An oxidation peak at 0.33 V is due to the oxidation of dopamine to o-dopaminoquinone and the reduction peak located at 0.10 V is corresponded to the transformation of o-dopaminoquinone to dopamine. The redox peak with the anodic and cathodic one at -0.15 V and -0.32 V, respectively is related to reversible oxidation of leucodopaminochrome to dopaminochrome [28]. The currents for the redox waves decrease with the increase of potential scan numbers.

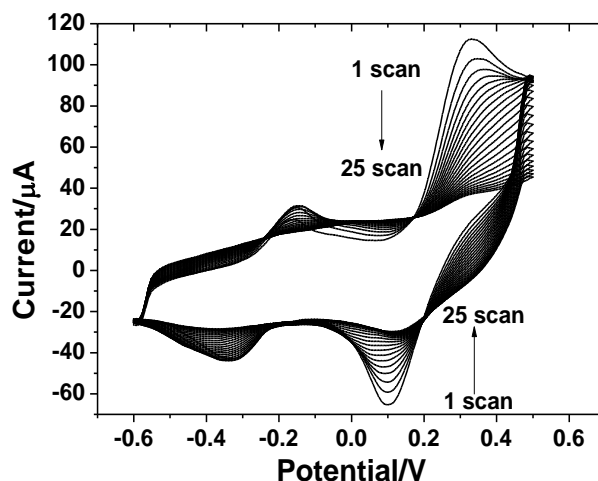


**Figure 1.** CVs of 5.0 mM dopamine for electropolymerization in a 60 mM pH 7.0 PBS, using a gold electrode at a potential scan rate of 0.1 V/s for 25 cycles.

The above results indicate that PDA film has been formed on the gold surface and the gold surface is passivated by the PDA film. Next, the PDA film modified gold electrode was undergone an overoxidation procedure by cycling the modified electrode in 0.5 M NaOH solution for six times. SEM was used to characterize the morphology of modified OPDA film. As observed from Fig. 2a, OPDA film appears a relatively rough and loose surface, which facilitating the immobilization of Au NPs. After electrodepositing Au NPs, flower-like nanoparticles can be observed in Fig. 2b, suggesting that Au NPs have been obtained. As shown in Fig. 2b, the particle size of the flower-like Au NPs are in the range of 50~100 nm.

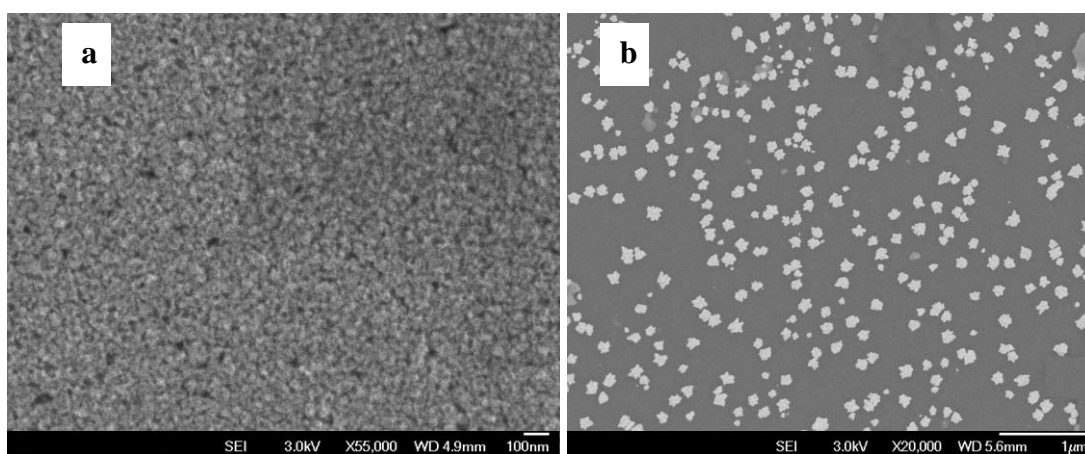


**Figure 2.** SEM images of (a) the OPDA modified gold electrode and (b) Au NPs/OPDA modified gold electrode.

### 3.2. EIS studies of different modified electrodes

EIS reveals the impedance variation of the electrode during different modification step. Fig. 3 shows nyquist plots of EIS obtained in 5 mM  $[\text{Fe}(\text{CN})_6]^{3-/4-}$  probe solution with 0.1 M KCl as

supporting electrolyte involved. 5 mV and 200 mV were respectively used as AC voltage amplitude and the imposed potential. The interface can be modeled by an equivalent circuit (shown in the inset of Fig. 3) as described in our previous work [29]. It is notable that the diameter of semicircular part at higher frequency is equivalent to the electron-transfer resistance ( $R_{et}$ ). As observed, for the bare Au electrode, the obtained  $R_{et}$  value was 550  $\Omega$ . While for the PDA/Au, the  $R_{et}$  value was decreased to 465  $\Omega$  due to the modification of conductive PDA film. After PDA was overoxidized to form OPDA film on the Au surface, a lower  $R_{et}$  value of 288  $\Omega$  was obtained. The subsequent loading of conductive Au NPs on OPDA surfaces makes the  $R_{et}$  value further decrease to 248  $\Omega$ , indicating a highly conductive modification has been deposited on electrode surface.

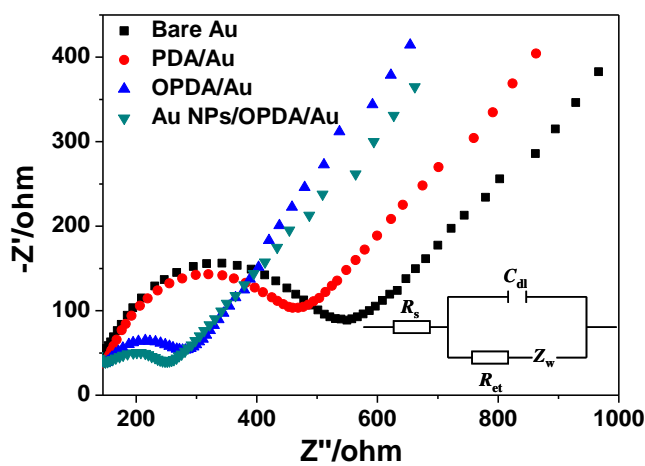


**Figure 3.** Nyquist plots of EIS obtained in 5 mM  $[\text{Fe}(\text{CN})_6]^{3-/4-}$  probe solution with 0.1 M KCl as supporting electrolyte involved.

### 3.3. Electrochemical response of Au NPs/OPDA modified electrode to $\text{H}_2\text{O}_2$

In order to investigate the electrocatalytic activities of Au NPs/OPDA modified electrode toward  $\text{H}_2\text{O}_2$  reduction, CVs for the bare Au electrode, Au NPs/Au, OPDA/Au and Au NPs/OPDA/Au in 1 mM  $\text{H}_2\text{O}_2$  were recorded. Fig. 4 shows the CVs of these modified electrodes in electrolyte of 0.1 M pH 7.0 PBS containing 1 mM  $\text{H}_2\text{O}_2$ . It can be observed that the onset potential for generating cathodic current is at -0.2 V for Au NPs/Au and OPDA/Au which is larger than that of the bare Au electrode, demonstrating that the immobilization of Au NPs and OPDA films on Au electrode surface enhanced its electrocatalytic activities to  $\text{H}_2\text{O}_2$  reduction. When the two materials of Au NPs and OPDA films were integrated together to form Au NPs/OPDA modified electrode, the onset reduction potential of  $\text{H}_2\text{O}_2$  on Au NPs/OPDA/Au is positively shifted to -0.1 V and the cathodic current of Au NPs/OPDA/Au is significantly the largest among the four electrodes. The onset reduction potential of  $\text{H}_2\text{O}_2$  on Au NPs/OPDA/Au is more positive than those of the ERGO-Ag (about -0.2 V vs Ag/AgCl) [30] and Ag-MnO<sub>2</sub>-MNCNTs composites electrode (about -0.2 V vs SCE) [31], indicating excellent electrocatalytic activities of Au NPs/OPDA toward reduction of  $\text{H}_2\text{O}_2$ . These results suggest that the OPDA films serving as Au NPs carrier generate additional electrocatalytic sites and synergetic effect toward electroreduction of  $\text{H}_2\text{O}_2$ . The electrocatalytic behavior of Au NPs/OPDA/Au toward various

concentrations of  $\text{H}_2\text{O}_2$  is investigated by CV and the results are shown in Fig. 5. The reduction currents are found to increase with adding concentrations of  $\text{H}_2\text{O}_2$  from 0 to 2 mM, which provides possibility for the following quantitative analysis.

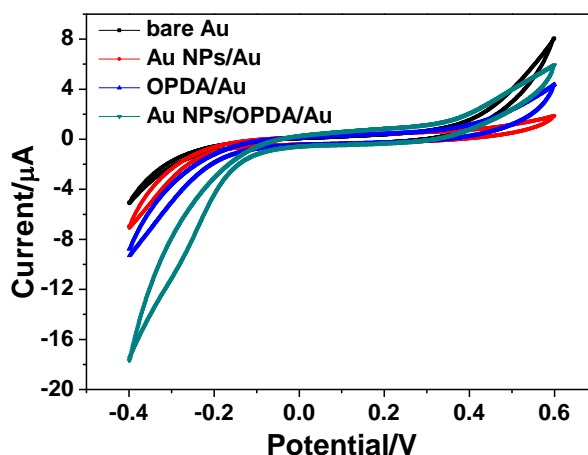


**Figure 4.** CVs of bare Au electrode, Au NPs/Au, OPDA/Au and Au NPs/OPDA/Au in electrolyte of 0.1 M pH 7.0 PBS containing 1 mM  $\text{H}_2\text{O}_2$  at a scan rate of 0.1 V/s.

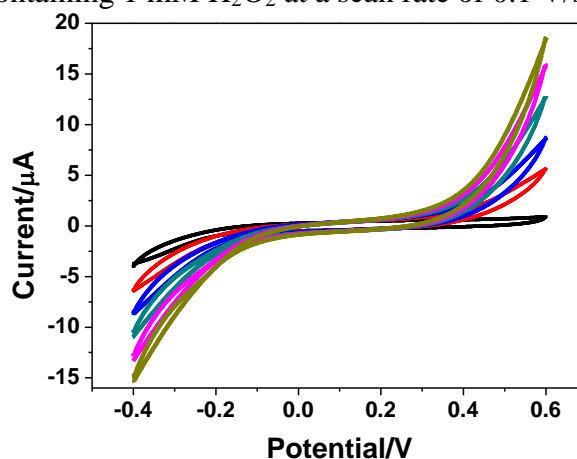


**Figure 5.** CVs of the Au NPs/OPDA/Au in electrolyte of 0.1 M pH 7.0 PBS with various concentrations (0, 0.4, 0.8, 1.2, 1.6, 2 mM) of  $\text{H}_2\text{O}_2$ .

To further confirm the possible synergism between OPDA film and Au NPs, the current-time responses for stepwise additions of 50  $\mu\text{M}$   $\text{H}_2\text{O}_2$  at an applied potential of -0.25 V were recorded for the above four electrodes. As shown in Fig. 6, compared to the bare Au electrode, Au NPs/Au and OPDA/Au, faradic current obtained on Au NPs/OPDA/Au is the largest and it is 75 times higher than that of bare Au electrode, illustrating the prominent electrocatalytic activities of Au NPs/OPDA/Au to the reduction of  $\text{H}_2\text{O}_2$ . Such improved electrocatalytic activities of the Au NPs/OPDA/Au is mainly ascribed to a possible synergism between OPDA film and the supported Au NPs, which contains high electrocatalytic sites for the  $\text{H}_2\text{O}_2$  reduction offered by the dispersed and uniform loading of Au NPs and accessible electron transfer channels provided by the loose OPDA films. Moreover, the OPDA films are used as a support in this work, which make the loaded Au NPs in a uniform distribution and avoid aggregation.

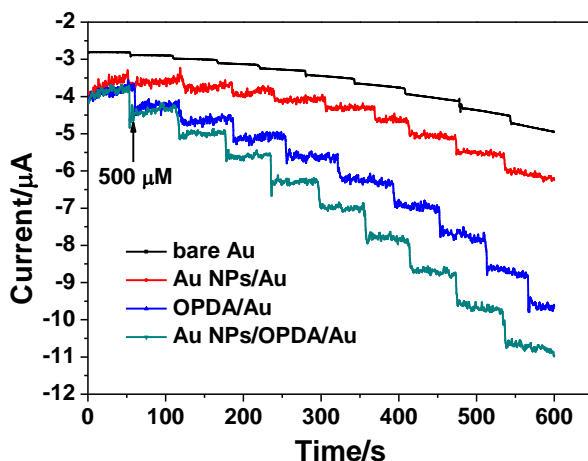


**Figure 6.** Current-time responses of the bare Au electrode, Au NPs/Au, OPDA/Au and Au NPs/OPDA/Au to stepwise addition of 50  $\mu\text{M}$   $\text{H}_2\text{O}_2$  in a stirred 0.1 mM PBS under a constant potential of -0.25 V.

3.4. Amperometric detection of  $\text{H}_2\text{O}_2$  at Au NPs/OPDA modified electrode

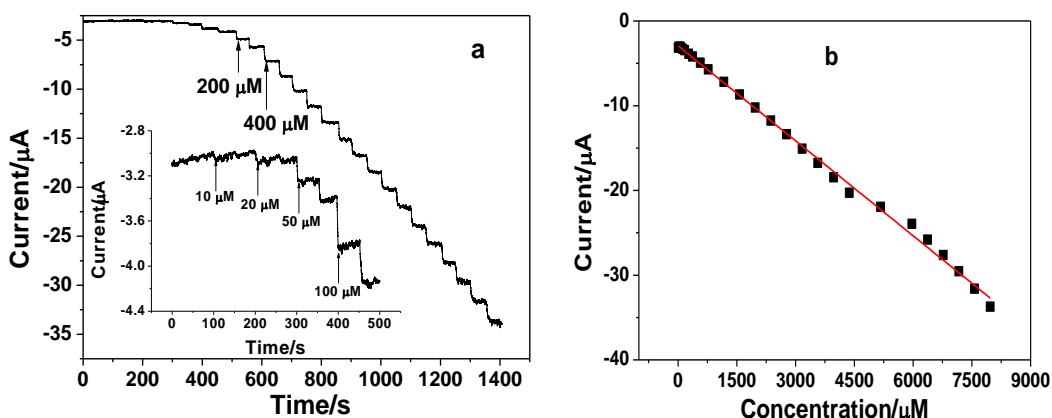


**Figure 7.** (a) Amperometric response of the Au NPs/OPDA/Au under a constant potential of -0.25 V on stepwise additions of various amounts of  $\text{H}_2\text{O}_2$  into stirring PBS (0.1 M, pH=7.0); (b) The linear relationship between electroreduction current of  $\text{H}_2\text{O}_2$  and its concentrations.

Rapid and precise  $\text{H}_2\text{O}_2$  detection capability of the Au NPs/OPDA modified electrode was evaluated by studying the amperometric responses upon the stepwise injection of different concentrations of  $\text{H}_2\text{O}_2$  under a constant potential of -0.25 V. As observed from Fig. 7a, the reduction currents of the Au NPs/OPDA/Au decrease gradually with the stepwise additions of  $\text{H}_2\text{O}_2$  into the stirring solution. The currents reach the steady-state within 3 s, demonstrating the rapid current response of the electrochemical sensor. The Fig. 7b shows the linear relationship between electroreduction current of  $\text{H}_2\text{O}_2$  and its concentrations. As observed, the obtained linear range of Au NPs/OPDA/Au spans the concentration of  $\text{H}_2\text{O}_2$  from 10  $\mu\text{M}$  to 8 mM with a detection limit of 0.5  $\mu\text{M}$  (SNR=3). The equation of linear regression is  $I (\mu\text{A}) = -2.93182 - 0.00374C (\mu\text{M})$  ( $R^2 = 0.99775$ ). The sensitivity of the sensor is calculated to be 52.94  $\mu\text{A mM}^{-1} \text{cm}^{-2}$ . Comparison of various  $\text{H}_2\text{O}_2$  sensing performances based on different nanomaterials is shown in Table 1. Obviously, the detection sensitivity obtained in this work is higher than the previously reported values at Ag nanowire (Ag NW,

26.6  $\mu\text{A mM}^{-1} \text{cm}^{-2}$ ) [8], Pt/PDA/RGO (13.3  $\mu\text{A mM}^{-1} \text{cm}^{-2}$ ) [13], gold nanoparticles/sulfonated graphene sheets (GNPs/SGS, 3.21  $\mu\text{A mM}^{-1} \text{cm}^{-2}$ ) [15] and  $\text{MnO}_2$ /graphene oxide (38.2  $\mu\text{A mM}^{-1} \text{cm}^{-2}$ ) [30] modified electrode. The linear range and detection limit is also comparable to other materials as listed in Table 1.

**Table 1.** Comparison of various  $\text{H}_2\text{O}_2$  sensing performances based on different nanomaterials.

Materials	Sensitivity	Linear ranges	Detection limit ( $\mu\text{M}$ )	Refs
Ag NW	26.6 $\mu\text{A} \cdot \text{mM}^{-1} \cdot \text{cm}^{-2}$	0.1 -3.1 mM	29.2	8
Pt/PDA/RGO	13.3 $\mu\text{A} \cdot \text{mM}^{-1} \cdot \text{cm}^{-2}$	0-1.0 mM	0.4	13
GNPs/SGS	3.21 $\mu\text{A} \cdot \text{mM}^{-1} \cdot \text{cm}^{-2}$	0.02-1.3 mM	0.25	15
PDA-Ag	6.79 $\mu\text{A} \cdot \text{mM}^{-1}$	0.092 -20 mM	1.97	17
$\beta$ - $\text{MnO}_2$ nanorods	21.74 $\mu\text{A} \cdot \text{mM}^{-1}$	0.00245-42.85 mM	2.45	21
$\text{MnO}_2$ /graphene oxide	38.2 $\mu\text{A} \cdot \text{mM}^{-1} \cdot \text{cm}^{-2}$	0.00 -0.6 mM	0.8	32
$\text{SiO}_2$ @Au-fibers-CS-HRP	-	0.005-1.0 mM	2.0	33
Au NPs/OPDA	52.94 $\mu\text{A} \cdot \text{mM}^{-1} \cdot \text{cm}^{-2}$	0.01-8 mM	0.5	This work

The selectivity is also an important factor for developing a high-performance  $\text{H}_2\text{O}_2$  sensor. For the present sensor, the selectivity was evaluated by investigating the influence of some potential coexistent species on the amperometric signal of  $\text{H}_2\text{O}_2$  at the proposed electrode. It was found that 100-fold of inorganic ions including  $\text{Mg}^{2+}$ ,  $\text{Ca}^{2+}$ ,  $\text{Fe}^{2+}$ ,  $\text{Cl}^-$ ,  $\text{SO}_4^{2-}$ , 10-fold of bio-related molecules, such as dopamine, ascorbic acid, glucose, and uric acid have no interference on  $\text{H}_2\text{O}_2$  detection, demonstrating good selectivity of the present method.

### 3.5. Stability and reproducibility of Au NPs/OPDA modified electrode

The amperometric signals of 0.1 mM  $\text{H}_2\text{O}_2$  at the modified electrode was determined during a month period at intervals of three days to investigate the stability of the proposed sensor. The results demonstrated that 93.8% of the initial current of the modified electrode was retained after storage for a month at room temperature, indicating an excellent stability. Furthermore, the reproducibility of the present modified electrode was investigated by determination of 0.1 mM  $\text{H}_2\text{O}_2$  using six independently prepared electrodes. It is found that a relative standard deviation (RSD) of 4.8% was obtained. Successive eight times determination of the electroreduction currents of  $\text{H}_2\text{O}_2$  at the same Au NPs/OPDA modified electrode resulted in a RSD of 2.1%. All of these results suggest that the Au NPs/OPDA modified electrode has the capability for a long-term and continuous analysis without losing its electrocatalytic activity significantly.

#### 4. CONCLUSIONS

In summary, the Au NPs/OPDA composites have been successfully prepared on gold electrode using an electrodeposition strategy. The obtained Au NPs/OPDA modified electrode presented a high electrocatalytic activity toward reduction of H<sub>2</sub>O<sub>2</sub> due to a possible synergism between the OPDA film and the Au NPs. The Au NPs/OPDA based H<sub>2</sub>O<sub>2</sub> sensor showed fast response (within 3 s), a wide linear range of 10 μM~8 mM, a low detection limit of 0.5 μM, a high sensitivity of 52.94 μA mM<sup>-1</sup> cm<sup>-2</sup> and acceptable selectivity.

#### ACKNOWLEDGEMENTS

This work was supported by the Grants from the National Natural Science Foundation of China (21105002), the fund project for Young Scholar sponsored by Henan province (2013GGJS-147), the Program for Science and Technology Innovation Talents at the University of Henan Province (14HASTIT012), and the Innovative Foundation for the College students of Anyang Normal University (ASCX/2015-Z14)

#### References

1. K.C. Lin, T.H. Tsai, S.M. Chen, *Biosens. Bioelectron.*, 26 (2010) 608.
2. A.C. Pappas, C.D. Stalikas, Y.C. Fiamegos, M.I. Karayannis, *Anal. Chim. Acta*, 455 (2002) 305.
3. A. Brestovisky, E. KirowaEisner, J. Osteryoung, *Anal. Chem.*, 55 (1983) 2063.
4. U. Pinkernell, S. Effkemann, U. Karst, *Anal. Chem.*, 69 (1997) 3623.
5. M. Abo, Y. Urano, K. Hanaoka, T. Terai, T. Komatsu, T. Nagano, *J. Am. Chem. Soc.*, 133 (2011) 10629.
6. T. Jiao, B.D. Leca-Bouvier, P. Boullanger, L.J. Blum, A.P. Girard-Egrot, *Colloids and Surfaces A*, 321 (2008) 137.
7. L. Wang, H. Zhu, H. Hou, Z. Zhang, X. Xiao, Y. Song, *J. Solid State Electrochem.*, 16 (2012) 1693.
8. E. Kurowska, A. Brzózka, M. Jarosz, G.D. Sulka, M. Jaskuła, *Electrochim. Acta*, 104 (2013) 439.
9. S. Yang, G. Li, G. Wang, J. Zhao, M. Hu, L. Qu, *Sensor Actuat. B-Chem.*, 208 (2015) 593.
10. K.F. Zhou, Y.H. Zhu, X.L. Yang, J. Luo, C.Z. Li, S.R. Luan, *Electrochim. Acta*, 55 (2010) 3055.
11. H. Yao, H. Liu, M. Sun, L. Gong, *Microchim. Acta*, 177 (2012) 31.
12. S.J. Li, J.M. Du, Y.F. Shi, W.J. Li, S.R. Liu, *J. Solid State Electrochem.*, 16 (2012) 2235.
13. Q.L. Zhang, T.Q. Xu, J. Wei, J.R. Chen, A.J. Wang, J.-J. Feng, *Electrochim. Acta*, 112 (2013) 127.
14. J.D. Qiu, H.Z. Peng, R.P. Liang, J. Li, X.H. Xia, *Langmuir*, 23 (2007) 2133.
15. S.J. Li, Y.F. Shi, L. Liu, L.X. Song, H. Pang, J.M. Du, *Electrochim. Acta*, 85 (2012) 628.
16. L. Wang, H. Zhu, H. Hou, Z. Zhang, X. Xiao, Y. Song, *J. Solid State Electrochem.*, 16 (2012) 1693.
17. A.J. Wang, Q.C. Liao, J.J. Feng, Z.Z. Yan, J.R. Chen, *Electrochim. Acta*, 61 (2012) 31.
18. S.J. Li, J.M. Du, J.P. Zhang, M.J. Zhang, J. Chen, *Microchim. Acta*, 181 (2014) 631.
19. A. Salimi, R. Hallaj, S. Soltanian, H. Mamkhezri, *Anal. Chim. Acta*, 594 (2007) 24.
20. D. Ye, H. Li, G. Liang, J. Luo, X. Zhang, S. Zhang, H. Chen, J. Kong, *Electrochim. Acta*, 109 (2013) 195.
21. A.J. Wang, P.P. Zhang, Y.F. Li, J.J. Feng, W.J. Dong, X.Y. Liu, *Microchim. Acta*, 175 (2011) 31.
22. F. Xu, M. Deng, G. Li, S. Chen, L. Wang, *Electrochim. Acta*, 88 (2013) 59
23. C. Wang, R. Yuan, Y. Chai, S. Chen, F. Hu, M. Zhang, *Anal. Chim. Acta*, 741 (2012) bbbbbb  
000000000000 15.

24. W. Hong, H. Bai, Y. Xu, Z. Yao, Z. Gu, G. Shi, *J. Phys. Chem. C*, 114 (2010) 1822.
25. A. Ma, Y. Xie, J. Xu, H. Zeng, H. Xu, *Chem. Commun.*, 51 (2015) 1469.
26. N. Zhang, W. Ma, P.G. He, Y.T. Long, *J. Electroanal. Chem.*, 739 (2015) 197.
27. C. Ruan, W. Shi, H. Jiang, Y. Sun, X. Liu, X. Zhang, Z. Sun, L. Dai, D. Ge, *Sensor Actuat. B-Chem.*, 177 (2013) 826.
28. T. Łuczak, *Electrochim. Acta*, 53 (2008) 5725.
29. S-J. Li, J-M. Du, J. Chen, N-N. Mao, M-J. Zhang, H. Pang, *J. Solid State Electrochem.*, 18 (2014) 1049.
30. B. Zhao, Z. Liu, W. Fu, H. Yang, *Electrochem. Commun.*, 27 (2013) 1.
31. Y. Han, J. Zheng, S. Dong, *Electrochim. Acta*, 90 (2013) 35.
32. L. Li, Z. Du, S. Liu, Q. Hao, Y. Wang, Q. Li, T. Wang, *Talanta*, 82 (2010) 1637.
33. J. Shen, X. Yang, Y. Zhu, H. Kang, H. Cao, C. Li, *Biosens. Bioelectron.*, 34 (2012) 132.

© 2016 The Authors. Published by ESG ([www.electrochemsci.org](http://www.electrochemsci.org)). This article is an open access article distributed under the terms and conditions of the Creative Commons Attribution license (<http://creativecommons.org/licenses/by/4.0/>).